JOURNAL OF Materials CHEMISTRY

The strength of colloidal interactions in the presence of ceramic dispersants and binders

Asad U. Khan,[a] Paul F. Luckham,*[b] Sivasegaram Manimaaran[b] and Murielle Rivenet[c]

[a]*Department of Chemical and Process Engineering, University of Surrey, Guildford UK GU2 7XH*
[b]*Department of Chemical Engineering, Imperial College of Science, Technology and Medicine, Prince Consort Road, London, UK SW7 2BY. E-mail: p.luckham01@ic.ac.uk*
[c]*ENSCL, Lab Cristallochim & Physicochim Solide, BP108, F-59652 Villeneuve Dascq, France*

Received 29th October 2001, Accepted 5th March 2002
First published as an Advance Article on the web 29th April 2002

In this study the interactions between an atomic force microscope (AFM) tip and a sapphire surface are investigated in the presence and absence of a dispersant, Aluminon, and a binder, poly(vinyl alcohol) (PVA). The results showed that attractive interactions are noted in the absence of the dispersant, but that these interactions become repulsive in its presence. Upon addition of binder to the system a weaker attractive interaction, which is preceded by a smaller repulsive interaction, is noted. The results of the AFM work are also compared to rheological studies that have been carried out on alumina dispersions stabilised by the aforementioned materials.

Introduction

In the past, the interactions between ceramic powders and the subsequent modification of their behaviour in the presence of dispersants has been investigated at a macroscopic level using well-established techniques such as rheology.[1–6] However, such techniques do not provide us with a definitive view describing the interactions at a particulate level. As such, other experimental techniques have had to be adopted for such a purpose. The work presented here is one such example, and attempts to bridge the gap between information gained at a macroscopic level with what occurs at a particulate level by making use of a relatively new tool—the atomic force microscope (AFM).[7] The AFM is currently the best tool available allowing one to determine the interactions that may occur between two particles.[8–10]

In the case of this study Aluminon, a dispersant, has been investigated both when acting alone, and then in combination with poly(vinyl alcohol) (PVA), a binder, so as to fully appreciate the mechanism by which it may stabilise a particular system. The binder is often used in ceramics to provide enough green strength, so that the green bodies can be moulded and retained in the desired shape without breaking, before sintering. Rheological data obtained from a Bohlin rheometer are compared with data obtained at a nano scale using a Topometrix Explorer AFM.

Experimental

Materials

Alumina AES-11 obtained from Mandoval Ltd., Surrey, UK was used in this work. It was obtained at 99.8% purity, had a Brunauer–Emmett–Teller (BET) surface area of 8.14 $m^2\ g^{-1}$ and a mean particle size of 0.4 μm. The suspensions used in the rheological experiments were composed of 40% by volume of alumina. De-ionised water was used to prepare the suspensions. As sub-micron powder material such as alumina forms agglomerates when stored, the agglomerates must be broken down as far as possible into the primary particles in order to prepare a homogeneous suspension. The methods used to prepare samples for this study included ball milling and ultrasonication.

The dispersant used for the purpose of this work is the ammonium salt of aurintricarboxylic acid, which is commonly referred to as Aluminon ($C_{22}H_{23}N_3O_9$). It is essentially an ammonium salt of an aromatic carboxylic acid. Its molecular structure is shown in Fig. 1 below and was purchased from Fluka Chemicals Ltd., UK with an active content >95%.

Poly(vinyl alcohol) (PVA) was used as the binding material in this work. It was obtained from Harlow Chemical, UK, and has a molecular weight of 61 000. It had a degree of hydrolysis ⩾98% and an active component content of 100%. Before using this polymer in the suspensions, a solution of concentration 10% w/v was prepared. The samples were generally dispersed using an ultrasonicator, but ball milling was also used on occasion.

The AFM work used a sapphire (alumina) surface obtained from Goodfellows Metal Plc., Cambridge.

Nanopure water was used for both preparing the solutions for the AFM experiments and for cleaning the surfaces.

Atomic force microscope

Atomic force microscopy (AFM) has in recent years become a standard technique for the imaging of surface topographies in both industry and academia. However, the AFM can also be used as a force-sensing tool to determine the strength of the

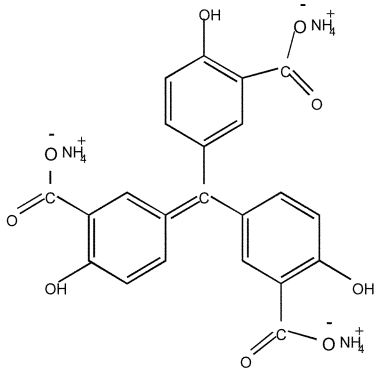

Fig. 1 Molecular structure of aurintricarboxylic acid ammonium salt (Aluminon).

interactions between an AFM tip and a surface in a given medium. The apparatus used here was a Topometrix explorer atomic force microscope (now Therma Microscopes), which was used in the 'force spectroscopy' mode.

In atomic force microscopy, a small soft cantilever is used to sense the forces at an interface. The lever–surface separation is controlled by a piezo-electric ceramic to nanometer resolution, and the deflection is determined using optical beam deflection. Beam deflection is intrinsically vibration tolerant (due to its inherent gain) and is relatively immune to contaminants and the media used compared to other techniques.[7] A split, four-quadrant, position-sensitive detector (PSD), monitors the beam deflection. This allows both the vertical and lateral spot motions to be resolved (*i.e.* the twisting as well as the bending of the lever). Data were captured using the standard Topometrix software, but all processing thereafter was done off line on commercial spreadsheet software. The force resolution of the set up was of the order 100 pN. The AFM lever is driven towards the surface by a piezo-ceramic at a rate of 1–10 nm s^{-1}. In this way force–distance profiles between the AFM tip and surface can be determined. In this study a commercial silicon nitride AFM tip with a tip radius of $\sim$50 nm and a spring constant of 0.03 N m^{-1} was used, and a flat sapphire disk was used as the lower, binding, surface.

Prior to each experiment, the lower, sapphire, surface was cleaned in a surfactant (RBS) solution followed by rinsing and further thorough cleaning in nanopure water so as to ensure the removal of any active agents on the surface. An ultrasonic bath was employed for the cleaning procedure. More often than not, a new tip was used for each experiment. However, when it was necessary to clean the tip, it was considered sufficient to rinse the tip repeatedly in ethanol and allow it to dry overnight. The ultrasonic bath was not employed in the case of the tip, as it was feared that such a procedure would damage the tip. After cleaning, the surfaces were then allowed to dry overnight in a laminar flow hood in a class 1000 clean room. The cleaned surfaces were then mounted on the AFM, and nanopure water injected in between the surfaces. This procedure was adopted as a matter of routine, as the results of the water experiment could be used to ascertain the cleanliness and therefore the suitability of the two surfaces for further experimentation. Appropriate, reproducible results at a number of sites on the sapphire surface were used as the guideline for further experimentation involving the surfaces in question.

Once satisfactory profiles were obtained in water, the water was drained away from the gap, and a solution of the dispersant being investigated was injected in between the surfaces. After allowing a sufficient amount of time for the system to equilibrate ($\sim$1 h), force measurements were then carried out on the system at a number of sites. Once again, reproducible results at a number of sites were seen to indicate the validity of the results.

Rheology

The rheological data reported here were obtained on a Bohlin VOR rheometer (Bohlin Reologi, Lund, Sweden). A concentric cylinder C25 measuring system was used here and the instrument can operate in both continuous shear and oscillatory shear mode.

In steady shear experiments, the sample was placed in the apparatus and the outer cylinder rotated at a known shear rate $\dot{\gamma}$. The resulting shear stress σ, was transmitted to the inner cylinder, which was connected to a transducer *via* an interchangeable torque bar (covering a wide torque range from 2.5×10^{-6} to 0.3 kg m^{-1}). Hence, the viscosity and shear stress can be measured as a function of shear rate.

$$\eta = \sigma/\dot{\gamma}$$

The computer interfaced with the rheometer controls all the shear rates and collects and analyses the data. The temperature of the sample was controlled by a water bath surrounding the outer cylinder. This water bath also dissipates any heat generated by the shearing of the sample. All measurements were made at 25 °C.

In this work, an alumina suspension was placed into the measuring cylinder and the system was sealed using a solvent trap so as to ensure minimal loss of water through evaporation and therefore changes to the volume fraction. The samples were initially sheared at very high shear rates (*ca.* 960 s^{-1}) for 3–4 minutes, and then allowed to equilibrate for at least 2 minutes before measurements were started. Measurements were conducted at both low and high shear rates (10^{-1}–10^{3} s^{-1}).

The viscoelastic properties of the system were characterised by measuring the maximum stress, σ_o, and strain, γ_o, amplitudes and the phase shifts. The main parameters here are the complex modulus G^*, the storage modulus G' and the loss modulus G'' where these are given by:

$$G^* = \tau_o/\gamma_o$$

$$G' = G^* \cos\delta$$

$$G'' = G^* \sin\delta$$

G' is a measure of the energy stored during a cycle of deformation and G'' accounts for the energy dissipated in the corresponding cycle.

Initial strain sweep measurements were performed by maintaining a constant frequency (1 Hz) while the strain amplitude, γ_o, was varied. The aforementioned parameters were measured as a function of γ_o in order to obtain the linear viscoelastic region. The values for G^*, G' and G'' remained constant with increasing γ_o until a critical strain γ_{cr} was reached. Upon reaching this, G^* and G' were seen to decrease while G'' increased. The region where G^*, G' and G'' are independent of the applied strain amplitude is referred to as the linear viscoelastic region. Measurements were conducted in this region as a function of frequency at constant strain.

Results and discussion

Fig. 2 illustrates the behaviour of the system in the absence of both dispersant and binder *i.e.* in the presence of nanopure water alone at a pH of $\sim$6.0, (note the pH is lower than 7.0 due to dissolved CO_2) The interaction profile shows a purely attractive force arising from the attractive van der Waals forces present in the system. The result can be used as evidence of the potential for aggregation in the absence of dispersant when ceramic powders are introduced into solution.

Fig. 3 through to 5 then show a typical set of profiles obtained at various time intervals for the interactions that result once a 1% by weight solution of Aluminon is introduced in between the two surfaces. The initial profile (Fig. 3) was

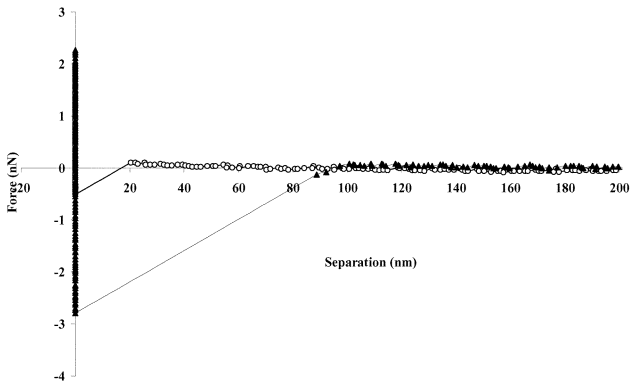

Fig. 2 Force–distance profile for silicone nitride tip with sapphire surface in nanopure water ○ on approach ▲ upon retraction.

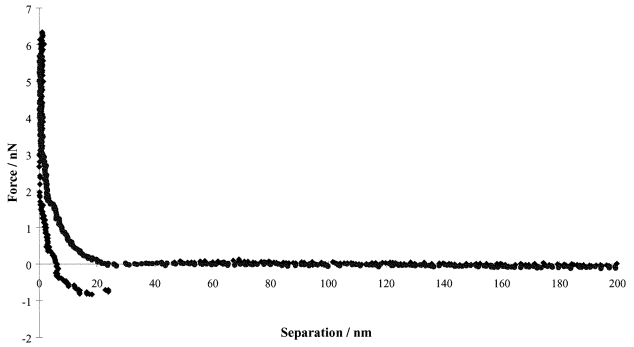

Fig. 3 Interaction between a sapphire surface and a silicon nitride AFM tip in the presence of Aluminon 1.5 h after the addition of Aluminon ● on approach ◆ upon retraction.

retrieved ~1.5 hours after sample injection and measurements were then repeated at a number of sites and on a number of subsequent occasions. The figure illustrates a very simple and effective result—the addition of Aluminon to the system results in the attractive forces being replaced by a purely repulsive interaction on approach, with the repulsive forces coming to the fore at a separation of 25 nm. As Aluminon is a rather large molecule, but not a polymer, it is believed that the repulsive forces must be electrostatic rather than steric in nature. However, there may be a very short-range (steric) barrier preventing an attraction in the form of the molecule itself lying adjacent to the surface. It can be noticed however, that a sizeable attractive component can be measured when the surfaces are separated. This is indicative of incomplete coverage of the surfaces, which could bring about aggregation in a real system at sufficiently high concentrations of the ceramic particles. At high concentrations in a dispersion, the particles will be forced closer to one another and were they to touch, the attractive forces would keep them in contact.

Fig. 4 shows the interactions 4 hours after the introduction of Aluminon. The repulsive interaction is somewhat longer ranged and now comes into play at ~35 nm, but more significantly, an attractive force component is no longer observed on retraction. The combination of an extended range of repulsion together with the absence of an attractive force component on retraction is indicative of complete or at least superior coverage of the surfaces by the Aluminon molecules after 4 hours. This also confirms the possibility of incomplete coverage 1.5 hours after injection.

Fig. 5 then shows the interaction profile after 6 hours and at this stage, little distinguishes the profile from those retrieved after 4 hours. Measurements taken after longer time intervals also showed little or no changes to the interaction profiles. This appears to suggest that near complete coverage is achieved after 4 hours, and at this stage, the system is colloidally stable.

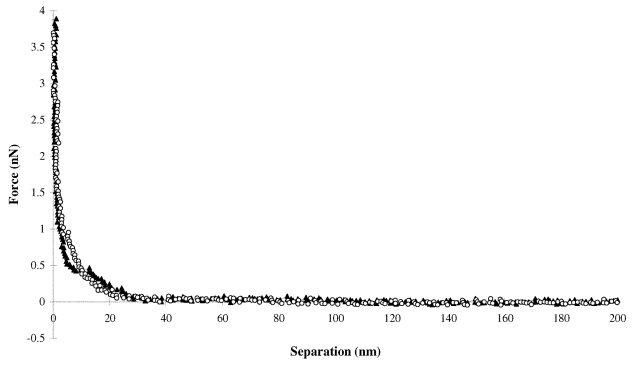

Fig. 4 Interaction between a sapphire surface and a silicon nitride AFM tip in the presence of Aluminon 4 hours after the addition of Aluminon ○ on approach ▲ upon retraction.

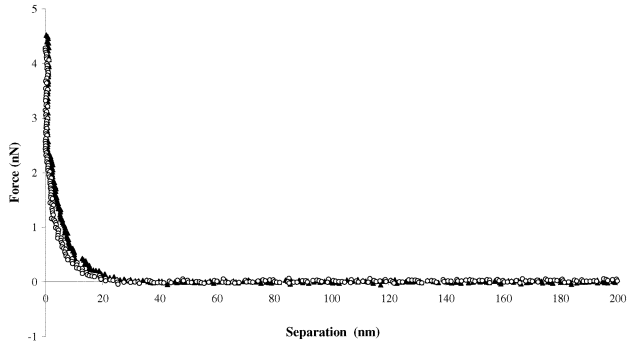

Fig. 5 Interaction between a sapphire surface and a silicon nitride AFM tip in the presence of Aluminon 6 hours after the addition of Aluminon ○ on approach ▲ upon retraction.

By way of comparison, Fig. 6 shows the variation in the viscosity of an alumina suspension in the presence of various amounts of the dispersant, Aluminon. The plot shows an initial decrease in the viscosity of the suspension with increasing Aluminon concentration as a result of the large aggregates otherwise present in the system being broken down. This initial drop is consistent with AFM observations (Fig. 3) as incomplete coverage by Aluminon particles leads to aggregation, as indicated by the attractive well in Fig. 3, thereby leading to the higher measured viscosities. An optimal concentration of about 0.25 wt/wt% is required for complete stabilisation and therefore the lowest measured viscosities. Under such circumstances, there is complete coverage of the particles and little or no free dispersant in the bulk solution. Adsorption isotherms confirm this finding (not shown here[11]). Here, the interaction between the particles will also be purely repulsive, be it on approach or retraction. Screening of the double layer then brings about the subsequent increase in the viscosities with further increases to the Aluminon concentration above 0.25 wt/wt%. Once complete surface coverage is achieved, increasing the Aluminon concentration increases the equilibrium bulk concentration of the dispersant. These dispersant molecules act as a free electrolyte in the suspension, which compress the electrical double layer responsible for stabilising the system. By increasing the ionic concentration, the double layer repulsion can be decreased to a range where the van der Waals attraction dominates over the double layer repulsion, leading to flocculation and hence increased viscosities of the suspension.[12]

Fig. 7 then illustrates the interactions that result when a binder, in the form of ~1% by volume PVA, is introduced into a system that is already stabilised by Aluminon. A clear

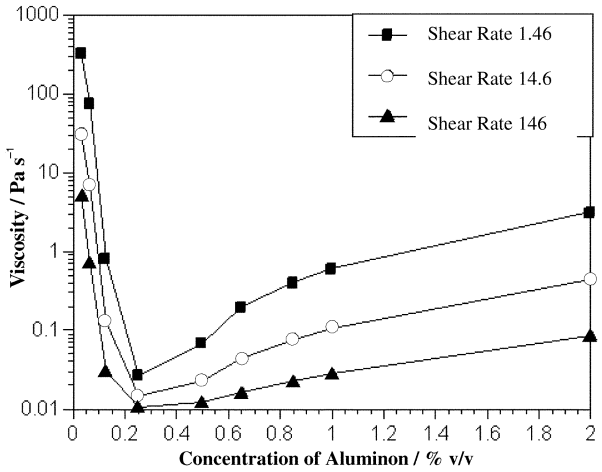

Fig. 6 Viscosity of alumina AES-11 40% v/v suspensions as a function of Aluminon concentration at various shear rates.

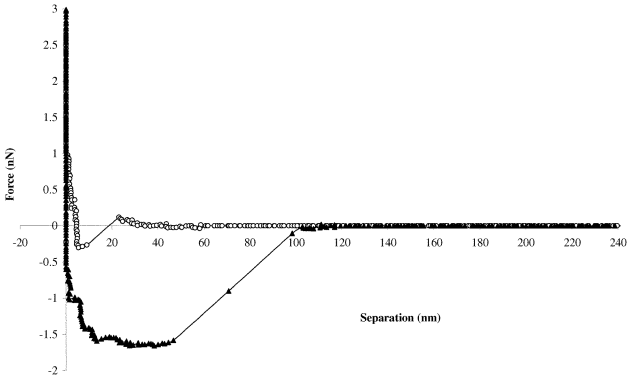

Fig. 7 Interaction between a sapphire surface and a silicone nitride AFM tip in the presence of Aluminon and PVA ○ on approach ▲ upon retraction.

difference can be identified in the force–distance profiles retrieved with PVA when compared to those retrieved in its absence. In its absence, reducing the separation between the surface and the tip results in the measurement of a repulsive force, which sets in at a distance of ~35 nm. The strength of the repulsive interaction increases as the separation is decreased. In the presence of PVA however, a small repulsion is first observed and this sets in at a very similar separation to that seen in its absence. This may be indicative of the effect of Aluminon once more and may provide proof of there being little removal of Aluminon from the surfaces following the addition of PVA. The initial repulsive force is then followed by a strongly attractive interaction that must be the effect of the PVA added to the system. This offers strong evidence of there being a flocculation mechanism in operation and as Aluminon has not been displaced as evidenced by the initial repulsion; it is quite likely to have been brought about by depletion.[13] The possibility of bridging can also be safely discounted as the measurements were conducted over an extended period of time and no significant changes to the nature of the profile were noted. The strength of the depletion forces measured here are comparable to those measured by Milling and Biggs.[14]

A general equation for the force of interaction due to depletion, F_{dep}, between a spherical particle and a flat surface was developed by Fleer *et al.*[15,16] who used a mean field approach to demonstrate that for surface separations below twice the radius of gyration of the free polymer, the intervening space is occupied by pure solvent.

$$F_{dep} = \pi \left[\frac{\mu_1 - \mu_1^0}{v_1^0}\right](h+2a)(h-2\Delta)$$

where, $(\mu_1 - \mu_1^0)$ is the chemical potential of the solvent, v_1^0 is the solvent molecular volume, a is the radius of the sphere, h is the separation and Δ is the depletion thickness, which can be identified with the radius of gyration of the dissolved polymer coil.[17] The chemical potential can be calculated using the Flory–Huggins theory of polymer solutions[18]

$$\mu_1 - \mu_1^0 = -kT\left[(1-1/n)\varphi_2^b + \ln(1-\varphi_2^b) + \chi_{12}(\varphi_2^b)^2\right]$$

where, n is the number of segments in a chain, φ_2^b is the bulk polymer volume fraction, χ is the Flory–Huggins polymer–solvent interaction parameter and k is the Boltzmann constant.

Inserting values for the various parameters of a ~50 nm; Δ ~10 nm; n ~4000; φ_2^b ~0.01; v_1^0 ~0.3 nm^3; and χ ~0.48 results in the calculation of depletion forces that are an order of magnitude smaller than those measured here. However, this discrepancy is not too significant in the light of the fact that the AFM tip dimensions are variable and the sample volumes for AFM measurements are very small and thereby magnifying errors associated with the polymer volume fraction. This problem can be compounded by any evaporation during the equilibration stage of the experiment, as the sample is not in an enclosed environment. The equation for the depletion force is highly sensitive to the effects of the tip geometry and the volume fraction and as such an order of magnitude difference need not be viewed in too harsh a light.

In studying the rheology, it was noted that the addition of the PVA to the Aluminon stabilised alumina AES-11 suspension increases the viscosity of the suspension significantly. The order of addition of the PVA and the dispersant was found to have little or no effect on the resulting suspensions.[11] As the PVA concentration in the Aluminon stabilised alumina suspensions is increased from 0 to 0.5%, the viscosity, at all shear rates, increases sharply, but above 0.5% PVA concentration, the viscosity is virtually constant. The relative viscosity at the three different shear rates is shown in Fig. 8. The relative viscosity at all three shear rates increases with increases to the PVA concentration from 0 to 0.5%. For PVA concentrations above 0.5%, relative viscosity is seen to decrease.

It was found that Aluminon in the PVA–water solution (without the alumina) does not greatly change the rheology of the Aluminon–PVA–water system.[11] Therefore, one may conclude that there are no significant interactions between the PVA and the Aluminon molecules in water.

The increase of the viscosity and the viscoelastic properties (though not shown here, the two moduli, G' and G'', show behaviour similar to that seen for the viscosity[11]) as the PVA concentration is increased, indicates that the addition of PVA flocculates the Aluminon stabilised alumina AES-11 particles. As PVA is a non-adsorbing (or very weakly adsorbing[19]) polymer, flocculation due to bridging mechanisms can be discounted. The alumina particles in the presence of Aluminon are highly negatively charged as has been observed in the electrophoresis experiments.[11] Furthermore, the addition of KNO_3 enhances the flocculation rate of the system under discussion even further. Therefore, a flocculation mechanism due to the van der Waals attractive forces may also be safely discounted.

Conclusion

The results obtained from the AFM are remarkably compatible with rheological data obtained on a very similar system. Rheology points to a reduction in viscosity following the addition of dispersant, and a subsequent increase following the addition of binder. AFM results point to repulsive interactions replacing attractive ones following the addition dispersant, with the strength and nature of the repulsion becoming more pronounced with time, until equilibrium is reached after 4 hours. On addition of binder, an attractive component comes into play. Furthermore, the AFM data seems to confirm the

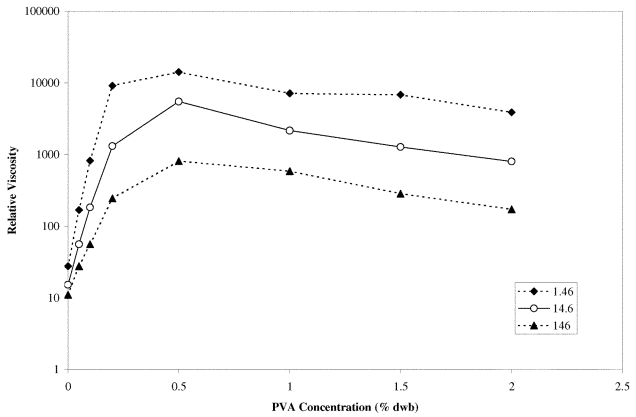

Fig. 8 Relative viscosity against PVA concentration, for Alumina AES-11 40% v/v suspensions stabilised with 0.25% Aluminon, at three different shear rates (1.46, 14.6 and 146 s^{-1}).

likelihood of depletion flocculation being the mode by which PVA re-flocculates a previously stabilised system. Though PVA is referred to as a binder in such systems, it does not appear to have adsorbed onto the surfaces.

References

1 W. Liang, Th. F. Tadros and P. F. Luckham, *J. Colloid Interface Sci.*, 1992, **153**, 131.
2 B. J. Briscoe, A. U. Khan, P. F. Luckham and N. Ozkan, in *Fourth Euro-ceramics*, ed. C. Galassi, Gruppo Editoriale Faenza Editrice S.p.A, Italy, 1995, vol. 2, pp 93–100.
3 B. J. Briscoe, A. U. Khan and P. F. Luckham, *J. Eur. Ceram. Soc.*, 1998, **18**, 2141.
4 B. J. Briscoe, A. U. Khan and P. F. Luckham, *J. Eur. Ceram. Soc.*, 1998, **18**, 2169.
5 A. U. Khan, B. J. Briscoe and P. F. Luckham, *Colloids and Surf. A*, 2000, **161**, 243.
6 S. Biggs, P. J. Scales, Y. K. Leong and T. W. Healy, *J. Chem. Soc., Faraday Trans.*, 1995, **91**, 2921.
7 G. Binnnig, C. F. Quate and Ch. Gerber, *Phys. Rev. Lett.*, 1986, **56**, 930.
8 W. A. Ducker, T. J. Senden and R. M. Pashley, *Nature (London)*, 1991, **353**, 239.
9 S. Biggs, *Langmuir*, 1995, **11**, 156.
10 B. Capella and G. Dietler, *Surf. Sci. Rep.*, 1999, **34**, 1.
11 A. U. Khan, PhD Thesis, Imperial College, 1997.
12 J. Israelachvili, in *Intermolecular and Surface Forces*, Academic Press, London, 1992, pp 213–254.
13 D. H. Napper, in *Polymeric Stabilisation of Colloidal Dispersions*, Academic Press, London, 1983, pp 378–412.
14 A. Milling and S. Biggs, *J. Colloid Interface Sci.*, 1995, **170**, 604.
15 J. M. H. M. Scheutjens and G. J. Fleer, *J. Phys. Chem.*, 1979, **83**, 1619.
16 J. M. H. M. Scheutjens and G. J. Fleer, *J. Phys. Chem.*, 1980, **84**, 178.
17 S. Asakura and F. Oosawa, *J. Chem. Phys.*, 1954, **22**, 1255.
18 P. J. Flory, in *Principles of Polymer Chemistry*, Cornell Univ. Press, Ithaca, NY, 1953, p 512.
19 B. C. Bonekamp, W. H. Van'T Van, M. J. Schoute and H. J. Veringain *EuroCeramic*, vol. I, G. de With, R. A. Terpstra and R. Metselaar (Eds.), Elsevier Applied Science, London 1989, p 145.